SUGISAKA MASANORI

Journal of Advances in Artificial Life Robotics
Vol. 4(3); December (2023), pp. 122–127
ON LINE ISSN 2435-8061; ISSN-L 2435-8061
https://alife-robotics.org/jallr.html

Research Article

Realizing Variable Stiffness through Structures Designed for Quick Motion

Katsuaki Suzuki[1], Yuya Nishida[2], Kazuo Ishii[2]
[1]*Kumamoto Industrial Research Institute, 3-11-38 Higashi machi, Higashi-ku, Kumamoto 862-0901, Kumamoto, Japan*
[2]*Life Science and Systems Engineering, Kyushu Institute of Technology, 2-4 Hibikino, Wakamatsu-ku, Kitakyushu 808-0196, Fukuoka, Japan*

ARTICLE INFO

Article History

Received 25 November 2022
Accepted 15 November 2023

Keywords

Variable stiffness
Link mechanism

ABSTRACT

To expand a robot's range of activities, we aim to realize three functions: normal motion, quick motion, and variable stiffness. In this study, we developed a method for realizing variable stiffness using a joint mechanism that can achieve normal and quick motions. Our analysis results confirmed that stiffness could be changed by adjusting the initial displacement of the spring incorporated in the joint mechanism. Furthermore, we manufactured a machine containing the proposed mechanism and evaluated the proposed method by comparing our theoretical and experimental results considering errors. Our findings showed similar trends between the measured and theoretical values with an error caused by friction between machine components.

1. Introduction

Various objectives can possibly be accomplished using robots with multiple functions, such as improving industrial productivity and robotic resource sampling in the deep sea. For multiple functions, our focus is on equipping robots with the ability to change the flexibility of their joints and be able to move quickly in the same way as humans do. Robots with these capabilities may be able to sample important marine resources, such as low-hardness minerals and fast-moving organisms, in extreme environments, such as the deep sea.

Actuators and joint mechanisms are core technologies for realizing these functions. The joint mechanism installed in an industrial robot generally combines a reducer with a single reduction ratio and a motor. In this paper, the motion achieved by this reducer–motor combination is defined as normal motion. Quick motion can be achieved using these mechanisms by increasing the motor output, but this increases the motor mass. Many studies are being conducted on mechanisms that combine actuators with springs to achieve quick motion while suppressing the increase in mass [1], [2]. However, these mechanisms do not include variable stiffness and are thus difficult to use for applications that require variable stiffness. Compliance control is commonly performed using force sensors to achieve stiffness change, but this approach has certain disadvantages, such as the difficulty of responding to external forces that exceed the control cycle [3]. Methods of achieving mechanical variable stiffness are also being investigated to solve the abovementioned problems [4], [5], [6]. However, these mechanisms do not discuss agile movements and are therefore hard to use for applications that need quick movements. In 2013, Nakamura et al. reported a joint mechanism that can achieve quick motion and variable stiffness using pneumatic artificial muscles [7], [8]. Although this joint mechanism can achieve two functions, it requires two pneumatic artificial muscles and one magneto rheological fluid brake and utilizes air pressure as its power source. Therefore, when these joints are used in autonomous field robots that investigate extreme

Corresponding author's E-mail: k-suzuki@kumamoto-iri.jp, y-nishida@lsse.kyutech.ac.jp, ishii@brain.kyutech.ac.jp

environments, installing a pneumatic tank or compressor is necessary, causing the robot to become larger.

We developed a joint mechanism that can perform normal and instantaneous movements to expand a robot's range of activities [9]. In the current paper, we add a feature to the abovementioned joint mechanism by developing a method of achieving variable stiffness using two motor drive methods while maintaining the existing mechanism structure.

2. Variable-stiffness function of proposed mechanism

Fig. 1 shows the process of changing the stiffness of an end effector. The proposed mechanism consists of an end effector, a main joint, a linear guide, a slider, a spring, two wires, two passive links, two cams, and two motors. Assume that the positions of the linear guide and main joint are fixed in space. Additionally, the linear guide and slider are a prismatic pair.

First, assume that the end effector angle θ_o of the state (a) is 0° and initial displacement of the spring is 0 (natural length). Further, assume that the brakes are acting on the two motors. When a load torque T_q is applied to the end effector and the end effector is rotated clockwise, the slider translates to the right via the wire, resulting in the state shown in (b). As the distance between the slider and main joint reduces, the spring is compressed to δ_{sp} and a compressive force F_{sp} is applied to the spring. When the X-direction forces of F_{sp} and F_w balance each other, the movement of each mechanical element stops; here, F_w is the tension applied by T_q.

Further, in the $\theta_o = 0°$ orientation, we consider a situation in which the two motors are rotated by the same angle but in different directions and initial spring displacement is ε_{sp}. Subsequently, brakes are applied to these two motors in a similar manner. Meanwhile, in state (c), F_{sp} acts on the spring and F_w acts on each of the two wires so that the forces are balanced. When the same magnitude of T_q as in the (b) state is applied to the end effector, the slider undergoes translational motion to the right, resulting in the (d) state. In the (c) state, because F_{sp} is already acting on the spring, compared to the (b) state, the slider only experiences slight displacement in the (d) state, enabling a balance between the X-direction force components of F_w and F_{sp}. Hence, the angular displacement of θ_o in state (d) is smaller compared to state (b), indicating that the stiffness of the end effector can be changed by adjusting ε_{sp}.

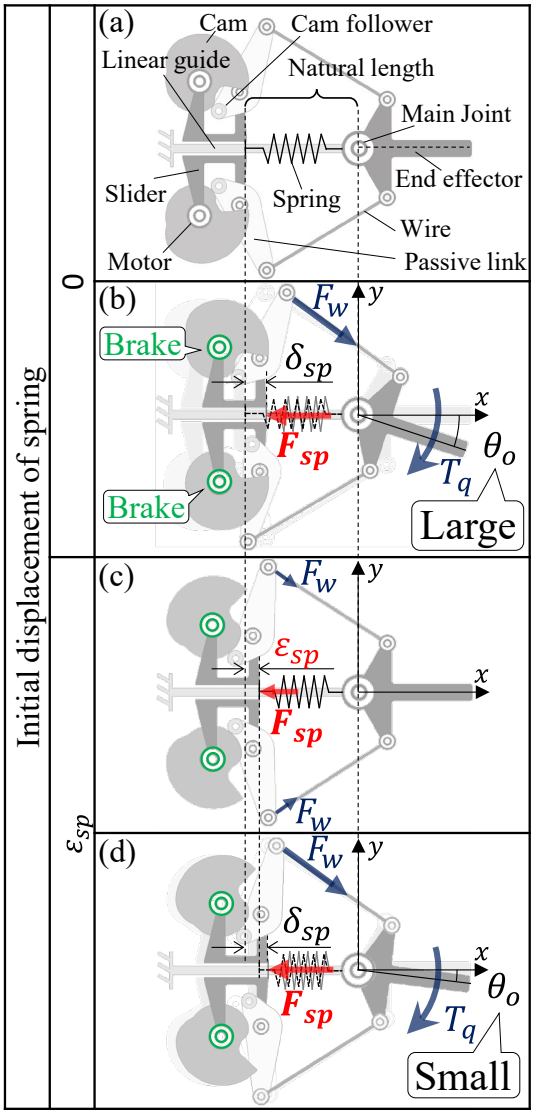

Fig. 1 Variable-stiffness function of proposed mechanism

3. Analysis of output characteristics related to stiffness

In the case of variable stiffness, we consider the load torque and the rotational stiffness of the end effector, which change with the initial displacement of the spring. Fig. 2 shows the link vectors of the proposed mechanism. The load torque applied to rotate the end effector should be of the same magnitude as the torque generated around the end effector due to internal force, such as wire tension. The relation between the load torque T_q and the internal force acting inside the mechanism is expressed as follows based on their geometric relation:

$$T_q = sign(\theta_o) k_{sp} \delta_{sp} l_l (-\sin\beta + \tan\theta_w \cos\beta). \quad (1)$$

Here, δ_{sp} is expressed by the following equation that employs the distance l_{spn} from the slider to the main joint when the spring possesses natural length and distance l_{sp} after displacement:

$$\delta_{sp} = l_{spn} - l_{sp}. \quad (2)$$

In Eq. (1), β is expressed as follows:

$$\beta = \begin{cases} \theta_o - \frac{\emptyset}{2} \ (\theta_o \geq 0) \\ -\theta_o - \frac{\emptyset}{2} \ (\theta_o < 0) \end{cases}. \quad (3)$$

Furthermore, the wire angles θ_w and passive link angle θ_m are expressed as follows based on their geometrical relation:

$$\theta_w = \sin^{-1}\left(\frac{l_s + l_m \sin\theta_m - l_l \sin\beta}{l_w}\right), \quad (4)$$

$$\theta_m = \cos^{-1}(\cos\theta_{mi} - \frac{\varepsilon_{sp}}{l_m}). \quad (5)$$

Fig. 3 shows the profile of the load torque T_q and angle θ_o of the end effector at initial spring displacements ε_{sp} of 0, 10, and 20 mm (Eq. (1)) [10]. Further, Table 1 shows the values of each parameter used in the analysis. When ε_{sp} is 0 mm, the magnitude of T_q changes continuously with respect to θ_o; however, when ε_{sp} is 10 and 20 mm, the magnitude of T_q changes quickly around 0°. This is because the compressive force preset in the spring changes with ε_{sp}. Therefore, stiffness can be changed considerably and instantaneously around θ_o = 0° by changing the magnitude of ε_{sp}.

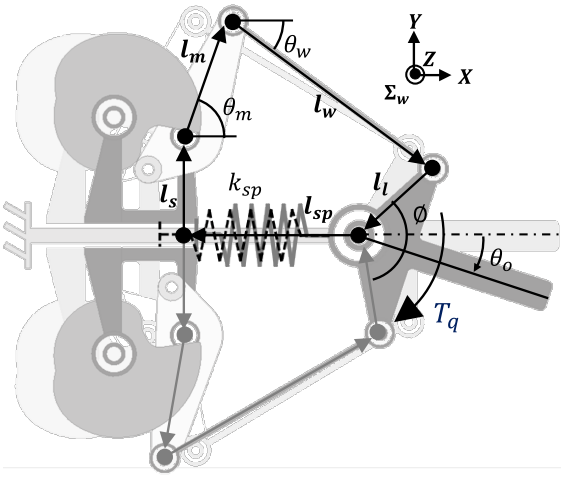

Fig. 2 Link vectors of the proposed mechanism

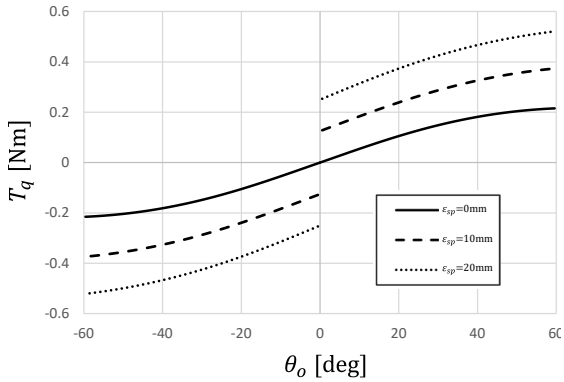

Fig. 3 Relation between the rotational angle of end effector and load torque

Table 1. Design parameters

k_{sp}	Spring constant	500 N/m
l_l	Length of $\boldsymbol{l_l}$	0.025 m
l_s	Length of $\boldsymbol{l_s}$	0.012 m
l_w	Length of $\boldsymbol{l_w}$	0.068 m
l_{spn}	Length of $\boldsymbol{l_{spn}}$	0.092 m
l_m	Length of $\boldsymbol{l_m}$	0.03 m
l_{cp}	Length of $\boldsymbol{l_{cp}}$	0.0181 m
$\emptyset$	Direction of $\boldsymbol{l_l}$	180°
$max(\theta_o)$	Maximum movement range	+60°
$min(\theta_o)$	Minimum movement range	−60°
θ_{mi}	Absolute angle of $\boldsymbol{l_m}$ when $\theta_o = 0, l_{sp} = l_{spn}$	36.3°

4. Design of experimental equipment

We built an experimental device to evaluate whether changing the initial displacement of the spring changes the rotational stiffness of the end effector of a real machine. Fig. 4 shows the designed and manufactured joint mechanism. The design parameters of the real machine are shown in Table 1. The real machine was designed to have a gripper-type structure in anticipation of future experiments related to object grasping and similar tasks. Its main structure is divided into four parts: a slider, the base, an output link and the end effector. The output link and end effector are connected via a spur gear mechanism. The reduction ratio of the spur gear mechanism is 1:1. Disregarding the friction between the spur gear and the bearing, the torque generated in the output link and end effector remains equivalent. Additionally, a worm gear is installed between the motor and cam. The worm gear is included to reduce power consumption when compressing the spring to maintain rigidity. The correspondence between the conceptual model of the joint mechanism and actual machine is shown in the cross-sectional view A in Fig. 4. The end effector in the conceptual model serves the same purpose the output link in the experimental equipment. The bottom image (side view) shown in Fig. 4 is the proposed mechanism mounted on and under the base. In other words, two mechanisms were built into the actual machine, and the two end effectors were controlled independently.

To evaluate the variable stiffness of the joint mechanism, we designed a device known as the load torque generator (Fig. 5) for applying a load torque to the end effector. The load torque generator comprises a link, motor, and fixed part. The fixed part is fastened to the base of the real machine such that the motor output shaft of the load torque generator and the rotary joint of end effector are coaxial. Moreover, the link of the load torque generator is attached to the end effectors.

Fig. 6 shows the experimental device system. First, 24 V DC power is supplied to a Maxon EPOS2 motor driver and the manufactured machine. The pulse values of the encoders mounted on the motors are sent to a PC via the EPOS2. The encoder pulse values obtained by the PC are used to solve the kinematics of the joint mechanism. Thereafter, a pulse width modulation signal is sent to the motor driver to control the angle of the motor's output shaft.

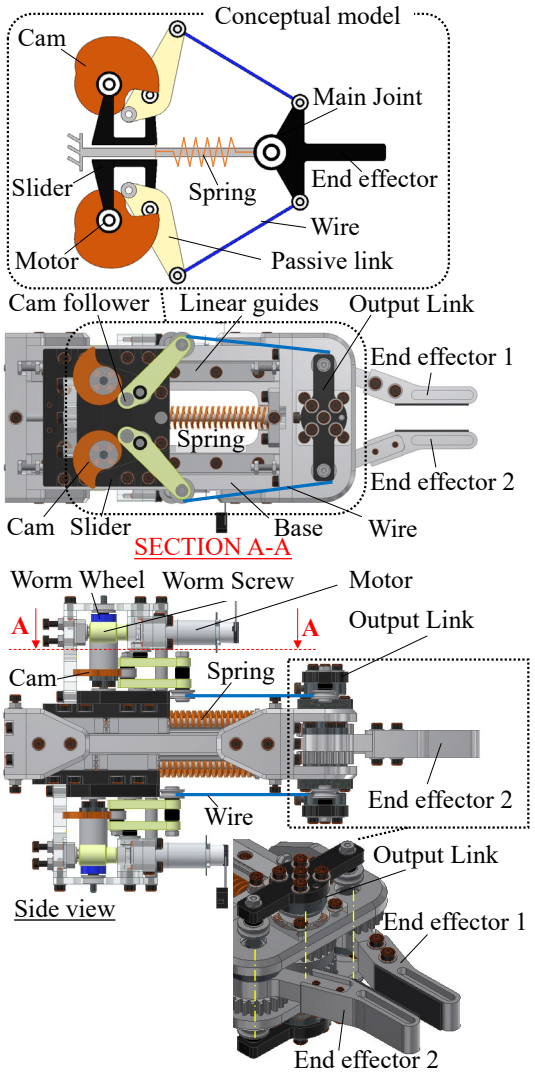

Fig. 4 Designed and manufactured machine

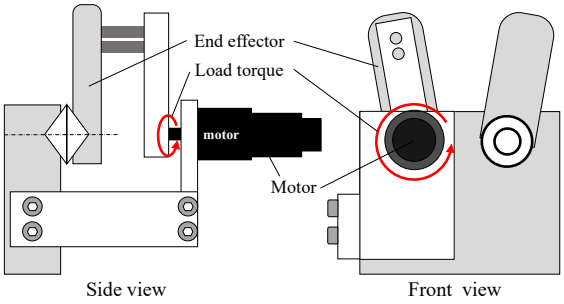

Fig. 5 Load torque generator

5. Experiments

Machines contain various component pairs, such as rolling pairs in linear guides and bearings and sliding pairs in spur gears, so the effects of friction between these pairs should be considered. However, frictional force is difficult to model and reflect in a theoretical formula. Therefore, to eliminate the effect of friction between component pairs, we applied load torque to the experimental device with the compression spring removed, and the load caused by friction was measured. Fig. 7 shows the relation between the load torque applied to the mechanism and the angle of the end effector. The results confirmed that the torque increased with the initial displacement of the spring. The reason for this was that the force acting on the linear guide increased in the thrust direction as the initial displacement of the spring increased because the angle between the wire and the passive link became acute. The measured results were linearly approximated, and a first-order approximation formula was derived (Fig. 7).

Next, we evaluated the variable stiffness of the joint mechanism with the springs by applying load torque to the end effectors. Fig. 8 shows four photos taken at 1-second intervals, while Fig. 9 shows the experimental results. The experiment was conducted by changing the initial displacement of the spring to 0, 10, and 20 mm. The rotational speed of the load motor was set to 500 rpm. The load torque caused by friction was subtracted from the measured value using the approximation formula shown in Fig. 7 because it is not considered in the theoretical formula. Consequently, the torque profiles of the experimental and calculated values exhibited roughly similar trends. On the contrary, the torque magnitude was larger in the experimental value than in the calculated value. This was because the compressive force acting on the spring enlarged the frictional force generated in each component pair when load torque was applied to the mechanism and the spring was displaced. In addition, the experimental results confirmed that a larger initial displacement of the spring led to a larger error between the calculated value and the real machine. This phenomenon was due to the same factors affecting the results in Fig. 7.

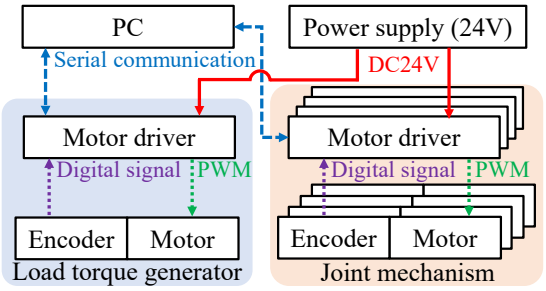

Fig. 6 Device system

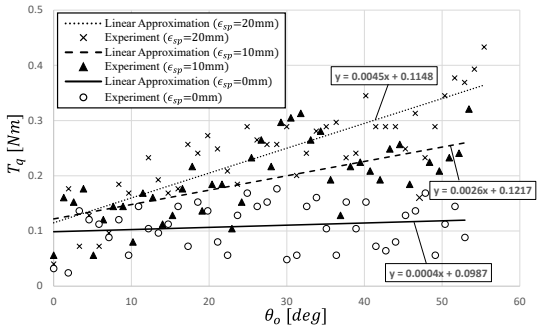

Fig. 7 Load torque and joint angle without internal spring

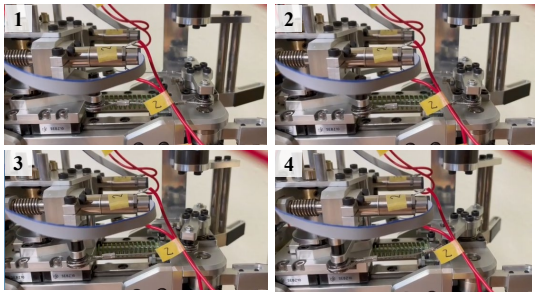

Fig. 8 Experiment situation

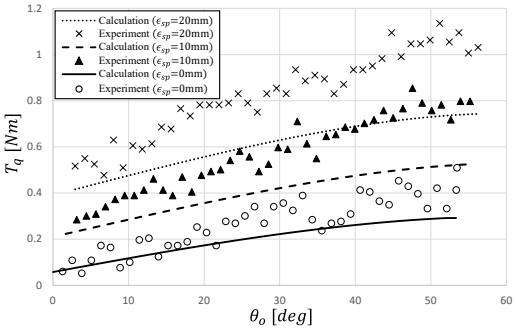

Fig. 9 Load torque and joint angle

6. Conclusion

In this study, we demonstrated a method for realizing variable stiffness using a joint mechanism that can perform normal and quick motions. Additionally, we derived a relational expression between the joint angle and the load torque applied to the end effector. The analysis results showed that the magnitude of the load torque required to rotate the end effector changed according to the initial displacement of the spring, thus changing the stiffness. Furthermore, we created an experimental device and measured the load torque and joint angle at different initial spring displacements. A comparison of the measured and theoretical values revealed that despite the friction-induced error in the magnitudes of the numerical values, the measured and theoretical values exhibit the same trends. Therefore, variable stiffness was achieved using the proposed mechanism by adjusting the initial displacement of the spring. One of the challenges here is to obtain a link length parameter that allows for considerable changes in stiffness. Another important issue is to reduce the frictional force acting on the prismatic and revolute pairs inside the mechanism. Further, improving the structure of the link mechanism is necessary for changing T_q continuously from $\theta_o = 0°$, which will enable it to be used in various applications.

References

1. Nassiraei, Amir AF, et al. Realization of the rapid movements for the entertainment robots by using two new actuators “inertia actuatror” and “CAM charger”. In: ASME International Mechanical Engineering Congress and Exposition, 2006. p. 1291-1297.
2. Kovač, Mirko, et al. A miniature jumping robot with self-recovery capabilities. In: 2009 IEEE/RSJ International Conference on Intelligent Robots and Systems. IEEE, 2009. p. 583-588.
3. Hogan, N. Adaptive control of mechanical impedance by coactivation of antagonist muscles, IEEE Transactions on Automatic Control, 1984, 29.8: 681-690.
4. Koganezawa, Koichi; Inaba, Tomoya; Nakazawa, Toshiki. Stiffness and angle control of antagonistially driven joint. In: The First IEEE/RAS-EMBS International Conference on Biomedical Robotics and Biomechatronics, 2006. BioRob 2006. IEEE, 2006. p. 1007-1013.
5. Choi, Junho, et al. Design of a robot joint with variable stiffness. In: 2008 IEEE International Conference on Robotics and Automation. IEEE, 2008. p. 1760-1765.
6. Sonoda, Takashi, et al. Development of antagonistic wire-driven joint employing kinematic transmission mechanism. Journal of Automation Mobile Robotics and Intelligent Systems, 2010, 4: 62-70.
7. Nakamura, Taro; Tanaka, Daisuke; Maeda, Hiroyuki. Joint stiffness and position control of an artificial muscle manipulator for instantaneous loads using a mechanical equilibrium model. Advanced Robotics, 2011, 25.3-4: 387-406.
8. Tomori, Hiroki, et al. Variable impedance control with an artificial muscle manipulator using instantaneous force and MR brake. In: 2013 IEEE/RSJ International Conference on Intelligent Robots and Systems. IEEE, 2013. p. 5396-5403.
9. Suzuki, Katsuaki, et al. A new rotary actuator capable of rapid motion using an antagonistic cam mechanism. Journal of Advances in Artificial Life Robotics, 2020, 1.3: 143-151.
10. Suzuki, Katsuaki. Research on antagonistic wire-driven joints with rapid motion and variable stiffness functions, Ph.D. thesis, Kyushu Institute of Technology, 2021.

Authors Introduction

Dr. Katsuaki Suzuki

He is a Researcher at the Kumamoto Industrial Research Institute, Japan. He received his Ph.D. degree from the Kyushu Institute of Technology in 2021. His research interests include joint mechanisms and their applications.

Dr. Yuya Nishida

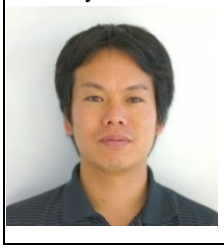

He is an Associate Professor at the Graduate School of Life Science and System Engineering, Kyushu Institute of Technology, Japan. His research interests include filed robotics, its application, and data processing.

Prof. Kazuo Ishii

He is a Professor at the Graduate School of Life Science and System Engineering, Kyushu Institute of Technology, Japan. His research interests include field robots and intelligent robot systems.